IOSR Journal of Applied Physics (IOSR-JAP)
e-ISSN: 2278-4861.Volume 8, Issue 1 Ver. III (Jan. - Feb. 2016), PP 42-46
www.iosrjournals

Correlation Of Optical Transmittance With Number Of Graphene Layers

Benjamin M. John[1,2], Simon W. Mugo[1], Nelson S. Timonah[1], Paul K. Ngumbi[1,2] and Ngei K.[1]

[1](Department of Physics, Jomo Kenyatta University of Agriculture and Technology (JKUAT), Nairobi Kenya)
[2](Department of Physics and Electronics, South Eastern Kenya University (SEKU), Kitui Kenya)

Abstract: *Optical transmittance of exfoliated multilayer graphene (MLG) was investigated and cross-referenced with a monolayer purchased from Graphene Supermarket USA, #Y060515. The transmittance was found to decrease exponentially with increase in the number of layers. Plots of grayscale values against position on the images from the thinnest edge generated step-like profiles. From the analysis of step heights and step widths, the transition from MLG to bulk graphite occurred at approximately 80 layers. The variations in step heights and step widths with position were attributed to the pressure differences on the surface of the samples during exfoliation, as well as the interlayer interactions within the samples. Our experimental results presented optical transmittance of 97.28, 95.23, 93.23, and 91.28% for a monolayer, bilayer, trilayer and tetralayer respectively. The observed decrease in transmittance with the number of graphene layers is attributed to the variations in optical absorption and reflection of the incident light by the MLG samples.*

Keywords: *Multilayer graphene, monolayer, optical microscopy, transmittance, image contrast.*

I. Introduction

The optical and electronic properties of two-dimensional (2D) layered nanomaterials such as graphene, MoS_2, BN, $MoSe_2$, WS_2, WSe_2, and $NbSe_2$ are highly dependent on their thickness [1-3]. The extraordinary optoelectronic properties of graphene results from its exceptional electronic structure in which valence and conduction bands touch each other at the K and K' points of the Brillouin zone, thus creating a zero band-gap semiconductor [4, 5]. The electrons in graphene thus have a characteristic linear dispersion relation between their energy and momentum near these points hence behave as massless Dirac fermions [6, 7]. MLG consist of stacked graphene nanosheets with weak Van der Waal interactions between the planes and whose optoelectronic properties correlate with the number of planes and their stacking order [2, 8]. The optical transmission of light through MLG directly depends on the optical conductance of graphene [9-11]. Derivations show that optical conductivity of MLG is almost linearly proportional to the number of graphene layers in the visible spectrum. Assuming that the inter-atomic interactions between the layers are negligible, the optical transmission through MLG is a negative nonlinear exponential function of the form:

$$T(\omega) = \left(1 + 0.5 f(\omega) N \pi \alpha\right)^{-2} \qquad (1)$$

Where $f(\omega)$ is the correction coefficient estimated to be 1.13 for a monolayer at $550nm$ wavelength, $\pi = 3.14$, N is the number of graphene layers and $\alpha = e^2/\hbar c \approx 1/137$ is the fine structure constant [6]. The transmittance of graphene has been estimated to be a constant $T \approx 97.7\%$ with an accuracy of $\pm 1\%$ in the visible range of electromagnetic spectrum [12]. The transmittance decreases with increase in the number of layers. Graphene has an absorbance equal to the universal constant given by $\pi\alpha \approx 2.3\%$. Using this constant, the thickness of MLG can be estimated [12-14]. In addition, graphene has a negligible reflectance of $< 1\%$. Optical spectroscopy indicates that MLG has opacity of $2.3 \pm 0.1\%$ which is independent of wavelength and increases with number of graphene layers with each graphene layer adding opacity of 2.3% [12, 15]. The stacking configurations of MLG is predicted to have a strong influence on the optoelectronic properties such as the band structure, magnetic state, interlayer screening and spin-orbit coupling [16, 17].

The strong influence of the stacking order particularly on the low-energy electronic structure was recently experimentally demonstrated by infrared spectroscopy [18]. The Bernal (ABA) stacking configuration has been presumed in most of studies involving mechanically exfoliated MLG. This is due to the fact that this structure reveals the highest thermodynamic stability compared to the rhombohedral (ABC) structure, which exists in a metastable state [19-26]. According to Shou-en *et al*. [27], the absorption of incident light of $\lambda = 550nm$ is independent of the stacking configurations. This has been confirmed by setting the interlayer hopping parameters between the atomic sites in any two nearest sheets to be $t_1 = 0.12t$, $t_3 = 0.1t$, and

$t_4 = -0.04t$. This results from the effect of interlayer hopping on the band structure below the energy of t_1 around the Van Hove singularities [2, 27, 28].

Various techniques including Raman spectroscopy, atomic force microscopy (AFM), and high-resolution transmission electron microscopy (TEM) have been used in determining MLG thickness [29, 30]. However, these techniques involve instruments that are hardly available in most laboratories due to their high cost and sophistication. In this work, we report a facile, versatile and cost effective method for accurate determination of MLG thickness using optical microscopy. This method presents a huge promise as it could be further extended to other 2D layered nanomaterials such as MoS_2 and BN. The fast and low cost nature of our technique makes it an ideal candidate for a standard characterization tool in the fast growing field of graphene.

II. Materials And Methods

MLG flakes were prepared by mechanical exfoliation of Highly Ordered Pyrolitic Graphite (HOPG) block, grade SPI-1, #426HP-AB (SPI supplies, USA). The samples were cleaned with absolute ethanol (purity-99.5%) and deionized water and placed on clean Borosilicate (Pyrex) microscope slides and dried by blowing with pressurized air. An optical microscope, model *Labomed LX 400*, in transmission mode was used to acquire images of the MLG flakes. The incident light $(400 \le \lambda \le 800nm)$ emitted by a halogen lamp passed through a $1mm$ aperture embedded on the microscope, and detected by a CCD camera interfaced with a computer. The lamp power was maintained at a constant light intensity (level 9) throughout the process. Imaging software *PixelPro* was used to acquire 8-bit colour images at resolution 1920 - 1080 pixels. Using *ImageJ 1.48v*, the optical contrast difference between the sample regions was analyzed in terms of grayscale values and position (μm) . Optical image and grayscale values of the graphene monolayer mounted onto a Fluorine-doped Tin Oxide (FTO) substrate (purchased from Graphene supermarket USA #Y060515) were obtained and used as the standard in our experiments.

III. Results And Discussions

Optical images of exfoliated MLG flakes were obtained at magnifications 10, 40, and 100X (Fig. 1).

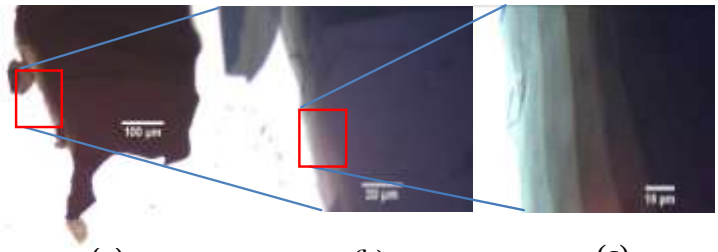

(a) (b) (c)

Figure 1: Optical images of MLG flakes at magnification (a) 10, (b) 40, and (c) 100X with clear contrast regions on the left hand side depicting differences in sample thickness. Clear optical contrast is at the edge of the flake image.

During mechanical exfoliation, the MLG layers snapped at the edges as depicted by the step-like profiles of grayscale values against position (Fig. 2c). The plots present step-like profiles of change in gray values with increase in distance along the dashed lines drawn on Fig. 2(a, b). The steps are as a result of variations in contrast and exhibit the layered nature of MLG samples. From each profile, step-height (h) and step-width (w) data values were extracted and plotted against position as shown in Fig. 3a and Fig. 3b, respectively.

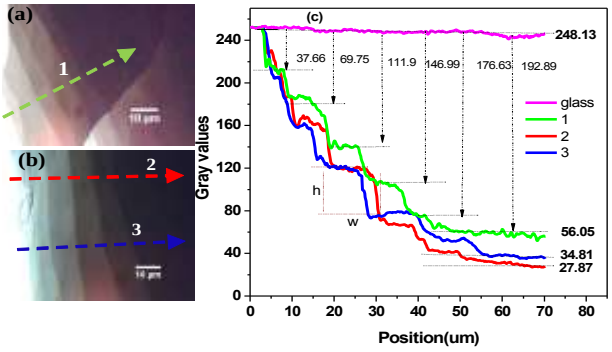

Figure 2: (a, b) Optical images of MLG samples showing directional line sections 1, 2, and 3 drawn perpendicular to the sample plane. (c) Profiles of contrast (gray values) as a function of position obtained along the dashed lines 1, 2, 3 and glass substrate.

The gray values varied from 248.13 – 56.05, 248.13 –27.87, and 248.13 –34.81 for profiles 1, 2, and 3, respectively. These values also decrease from 248.13 at the thinnest edge to 27.87, at the thickest region of the flake for profile 2. From the plot of step height against position (Fig. 3a), a distinct trend is observed in profiles 1, 2, and 3, where the step heights increases until they reach maximum grayscale values of 42.15, 51.25, and 44.30 for curves 1, 2, and 3, respectively. Beyond these values, the step heights decrease sharply. The maximum values, beyond which the step heights begins to decrease, correspond to 56, 93, and 88 layers for curves 1, 2, and 3, respectively. On average, the maximum values occur at a region with 80 layers [31].

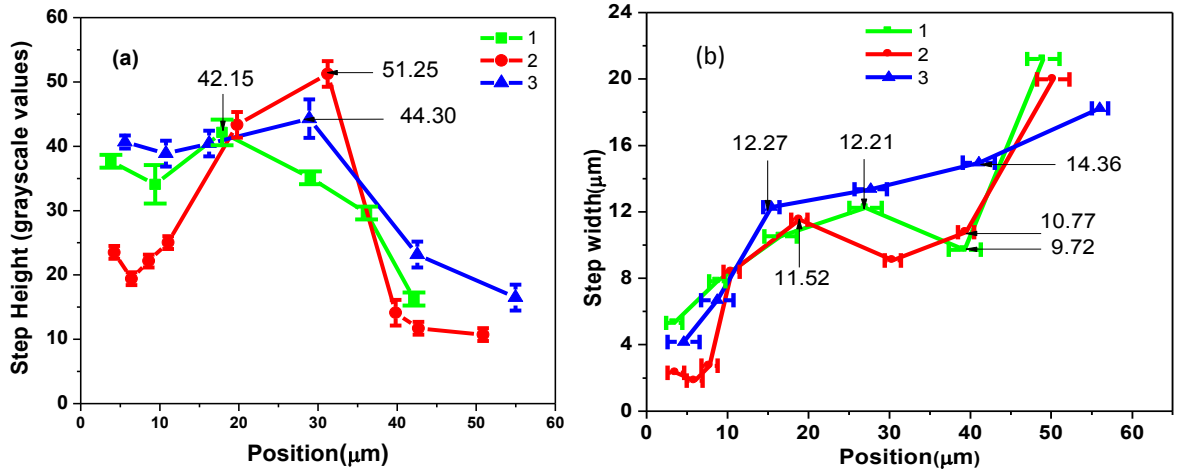

Figure 3: (a) Plot of measured step height values against position for profiles 1, 2, and 3 (shown in Fig. 2c). (b) Plot of measured step width values against position for profiles 1, 2 and 3 (shown in Fig. 2c).

From the plot of step widths against position (Fig. 3b), a sharp increase in step widths until points 12.21, 11.52, and 12.27μm for curves 1, 2, and 3, respectively was observed. At these points, curves 1 and 2 attains a negative slope while in curve 3, the gradient reduces significantly. At approximately 40μm from the edge, step widths 9.72, 10.77, and 14.36μm were observed. Beyond 40μm, the gradient of the curves increases sharply. The shortest step width of 1.84 μm was recorded at 5.93 μm in curve 2 whereas the longest step width of 21.20μm was recorded at 49.02μm in curve 1. The points with the lowest gradients correspond to 74 – 89, 67 – 93, and 66 – 88 layers for curves 1, 2, and 3, respectively. These points were also determined to be at regions with 80 layers, which is within the MLG region [31].

The observed trend in step-heights and step-widths is attributed to the variation in atomic-scale strain in the carbon-carbon bonds in the sample and their interlayer interactions. Higher pressure is exerted on the edges than on the bulk of the MLG sample and therefore, most of the layers snaps at shorter distances from the thin edges. The weak non-covalent interaction of $\approx 43meV$ per atom between graphene sheets is low at the edges where the samples are ultrathin and increases with graphene layers [32]. This means that at the bulk of the MLG, the interactions are very high and therefore, the graphene sheets tend to resist the externally applied force leading to reduced snapping. Average gray values of the graphene monolayer were found to be 1.98 ± 0.005. Since each graphene layer contributes absorbance of 2.3% [12, 33], the conversion of these gray values, based on Beer Lambert's Law, show transmittance of 98.23%. The cumulative grayscale value differences at each step in MLG samples were further converted into transmittance and a model in form of a plot of transmittance against number of MLG layers developed (Fig. 4).

From the plot (Fig. 4), the optical transmittance of the MLG decayed steadily with the sample thickness. At the edges of the samples, the optical transmittance was recorded as; 71.19, 80.88, and 65.61% for profiles 1, 2, and 3 respectively while on the bulk regions, it was recorded as; 17.52, 16.56, and 16.36% for profiles 1, 2, and 3, respectively.

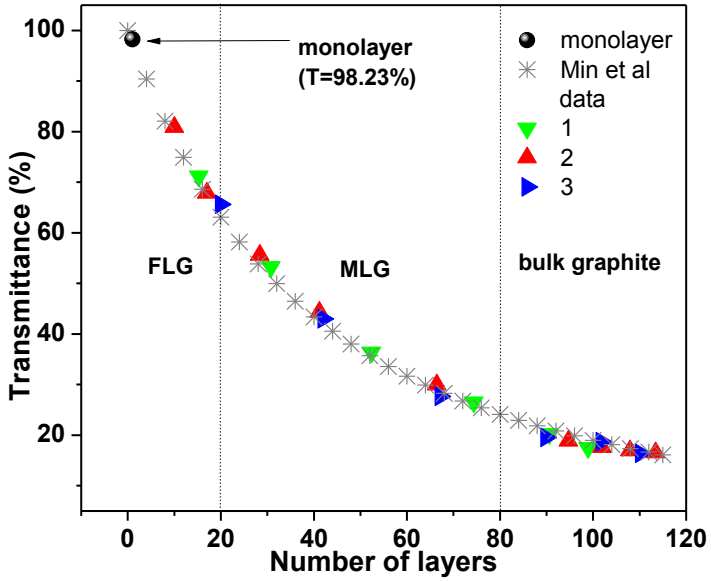

Figure 4: Optical transmittance of exfoliated MLG samples. The experimental data points were extracted from profiles 1, 2 and 3 in Fig. 2c.

Fig. 4 shows a model developed from the data obtained from the profiles in Fig. 2c. From the model, the relation between the optical transmittance and the sample layers was found to be governed by the negative non-linear exponential function (equation 2);

$$T = 89.38e^{-N/42.17} + 9.99 \qquad (2)$$

Where T and N represent transmittance and number of layers respectively. From the model, the optical transmittance of a monolayer was found to be $97.28 \pm 0.005\%$, which is comparable with the estimated 98.23% optical transmittance of the standard monolayer sample. The optical transmittance decreases with increase in the number of graphene layers. For example; we obtained transmittance of 95.23 ± 0.005, 93.23 ± 0.005, and 91.00% for bilayer, trilayer, and tetralayer, respectively. From Min and Macdonald [9] simulation (equation 1), the obtained optical transmittance was 97.46, 95.01, 92.65, and 90.38% for a monolayer, bilayer, trilayer and tetralayer respectively, with an error of $\pm 0.005\%$ The experimental results thus agree with Min and Macdonald [9] theoretical simulation results with a slight deviation of about $\pm$ 1%. The experimental results also match well with Shou-en *et al*. [27] data on optical transmission of MLG grown through CVD.

The observed trend is as a result of the variation in absorption of light in the MLG sheets. At regions with few layers, where transmittance is very high, the graphene sheets transmit light with relatively little absorption and reflection. The absorption and reflection of light in this case increases with the sample thickness. The observed discrepancy may be attributed to hydrocarbon contaminations such as organic residue and dust, or disorders such as carbon vacancies which may have been present in the samples. Our model therefore, provides a fast and reliable way of estimating the number of graphene layers in MLG samples which can be achieved by simply measuring their optical transmittance and fitting the results in equation 2.

IV. Conclusion

From the analysis of step heights and step widths, we found that the transition from MLG to bulk graphite occurred at around 80 layers. We have modelled the analytical expression (Equation 2) for determining number of graphene layers by obtaining optical transmittance of the MLG samples. From the expression, the optical transmittance of a given MLG sample would be 98.28, 95.23, 93.23, and 91.00 for a monolayer, bilayer, trilayer, and tetralayer, respectively, with an error of ± 0.005. The number of layers in the MLG samples varied from 11 to 114. This work shows that, optical microscopy offers a quantitative solution to identification and counting of MLG layers. Optical microscopy is a facile, versatile and reliable technique which can be applied in any standard laboratory equipped with a microscope and CCD or a digital camera. This technique can be extended to the other 2D layered nanomaterials with weak Van der Waals interlayer interaction such as MoS_2, BN, $MoSe_2$, WS_2, WSe_2, $NbSe_2$, TiS_2 and TaS_2.

References

[1] L. Hai, W. Jumiati, H. Xiao, L. Gang, Y. Jian, L. Xin, X. Qihua and Z. Hua, Rapid and Reliable Thickness Identification of Two-Dimensional Nanosheets Using Optical Microscopy, ACS Nano, 7(11), 2013,10344-10353.

[2] F. M. Kin, L. Changgu, H. James, S. Jie and F. H. Tony, Atomically thin MoS2: A new direct-gap semiconductor, Physical Review Letters, 105, 2010, 136805.

[3] A. H. Castro, F. Guinea, N. M. R. Peres, K. S. Novoselov and A. K. Geim, The electronic properties of graphene, Review of Modern Physics, 81(1), 2009, 109-162.

[4] P. R. Wallace, The Band Theory of Graphite, Physical Review, 71(9), 1947, 622-634.

[5] J. C. Slonczewski and P. R. Weiss, Band Structure of Graphite, Physical Review, 109(2), 1958, 272-279.

[6] A. K. Geim, Graphene: Status And Prospects, Science, 324(5934), 2009, 1530-1534.

[7] Y. B. Zhang, Y. W. Tan, H. L. Stormer and P. Kim, Experimental observation of the quantum Hall effect and Berry's phase in graphene, Nature, 438, 2005, 201-204.

[8] M. I. Katsnelson, Graphene; Carbon in Two Dimensions (Cambridge: Cambridge University Press, 2012)

[9] H. Min and A. H. MacDonald, Origin of universal optical conductivity and optical stacking sequence identification in multilayer graphene, Physical Review Letters, 103(6), 2009, 067402.

[10] P. Avouris, Graphene: Electronic and photonic properties and devices, Nano Letters, 10(11), 2010, 4285–4294.

[11] A. B. Kuzmenko, E. van Heumen, F. Carbone and D. van der Marel, Universal optical conductance of graphite, Physical Review Letters, 100(11), 2008, 117401-4.

[12] R. R. Nair, P. Blake, A. N. Grigorenko, K. S. Novoselov, T. J. Booth, T. Stauber, N. M. R. Peres and A. K. Geim, Fine structure constant defines visual transparency of graphene, Science, 320(5881), 2008, 1308.

[13] L. A Falkovski, Optical properties of graphene, Journal of Physics, Conference Series, 129(1), 2008, 012004-4.

[14] L. A. Falkovsky, and A. A. Varllamov, Space-Time dispersion of graphene conductivity, The European Physical Journal, B 56 (4), 2007, 281-284.

[15] V. P. Gusynin, S. G. Sharapov, and J. P. Carbotte, Unusual microwave response of Dirac quasiparticles in graphene, Physics Review Letters, 96(25), 2006, 256802.

[16] M. F. Craciun, S. Russo, M. Yamamoto, J. B. Oostinga, A. F. Morpurgo and S. Thrucha, Graphene. Carbon in Two Dimensions, Nature Nanotechnology, 4, 2009, 383-388.

[17] J. L. Manes, F. Guinea and M. A. H. Vozmediano, Existence and topological stability of Fermi points in multilayered graphene, Physical Review, B 75(15), 2007, 155424.

[18] W. Yingying, N. Zhenhua, L. Lei, L. Yanhong, C. Chunxiao, Y. Ting, W. Xiaojun, S. Dezhen and S. Zexiang, Stacking-Dependent Optical Conductivity of Bilayer Graphene, ACS Nano, 4(7), 2010, 4074-80.

[19] H. K. Min and A. H. MacDonald, Chiral decomposition in the electronic structure of graphene multilayers, Physical Review B, 77, 2008, 155416.

[20] H. K. Min and A. H. MacDonald, Electronic structure of multilayer graphene. Progress of Theoretical Physics Supplement, 176, 2008, 227–252.

[21] R. R. Haering, Band structure of rhombohedral graphite, Canadian Journal of Physics, 36(3), 1958, 352-362.

[22] F. Bassani and P. P. Parravicini, Electronic States and Optical Transitions in Solids, (1st Ed.) (New York: Pergamon Press, 1975).

[23] M. Koshino and T. Ando, Orbital diamagnetism in multilayer graphenes: Systematic study with the effective mass approximation. Physical Review, B 76(8), 2007, 085425.

[24] K. F. Mak, M. Y. Sfeir, J. A. Misewich and T. F. Heinz, The evolution of electronic structure in few-layer graphene revealed by optical spectroscopy. Proceedings of the National Academy of Science, 107(34), 2010, 14999–15004.

[25] K. F. Mak, S. Jie, and T. F. Heinz, Electronic structure of few-layer graphene: experimental demonstration of strong dependence on stacking sequence, Physical Review Letters, 104(17), 2010, 176404.

[26] J. C. Charlier, J. P. Michenaud and X. Gonze, First-principles study of the electronic properties of simple hexagonal graphite, Physical Review, B 46, 1992, 4531-4539.

[27] Z. Shou-en, Y. Shengjun and G. C. Janssen, Optical transmittance of multilayer graphene, EPL: Exploring the frontiers of physics, 108, 2014, 17007.

[28] F. Guinea, A. H. C. Neto and N. M. R. Peres, Electronic states and Landau levels in graphene stacks, Physical Review, B 73(24), 2006, 245426.

[29] A. C. Ferrari, J. C. Meyer, V. Scardaci, C. Casiraghi, M. Lazzeri, F. Mauri, S. Piscanec, D. Jiang, K. S. Novoselov, S. Roth and A. K. Geim, Raman spectrum of graphene and graphene layers, Physical Review Letters, 97(18), 2006, 187401.

[30] C. G. Lee, H. G. Yan, L. E. Brus, T. F. Heinz, J. Hone and S. M. Ryu, Anomalous lattice vibrations of single and few-layer MoS_2, ACS Nano, 4(5), 2010, 2695–700.

[31] J. D. Wadhawan and R. G. Compton, Electrochemistry-Eds (Cambridge: RSC Publishing Cambridge, 2013).

[32] R. Zacharia, H. Ulbricht and T. Hertel, Interlayer cohesive energy of graphite from thermal desorption of polyaromatic hydrocarbons, Physical Review, B 69, 2004, 155406.

[33] B. F. Claudia and M. L. Doroteo, Multilayer Graphene Synthesized by CVD Using Liquid Hexane as the Carbon Precursor, World Journal of Condensed Matter Physics, 1, 2011, 157-16.